Model-independent measurement of cosmic curvature with the latest $H(z)$ and SNe Ia data: A comprehensive investigation

Jing-Zhao Qi,[1] Ping Meng,[1] Jing-Fei Zhang,[1] and Xin Zhang[1,2,3,*]

[1]*Key Laboratory of Cosmology and Astrophysics (Liaoning Province) and Department of Physics, College of Sciences, Northeastern University, Shenyang 110819, China*

[2]*Key Laboratory of Data Analytics and Optimization for Smart Industry (Ministry of Education), Northeastern University, Shenyang 110819, China*

[3]*National Frontiers Science Center for Industrial Intelligence and Systems Optimization, Northeastern University, Shenyang 110819, China*

(Received 23 February 2023; accepted 18 August 2023; published 25 September 2023)

In the context of the discrepancies between the early and late universe, we emphasize the importance of independent measurements of the cosmic curvature in the late universe. We present an investigation of the model-independent measurement of the cosmic curvature parameter Ω_k in the late universe with the latest Hubble parameter $H(z)$ measurements and type Ia supernovae (SNe Ia) data. For that, we use two reconstruction methods, the Gaussian process (GP) and artificial neural network (ANN) methods, to achieve the distance construction from $H(z)$ data. Our analysis reveals that the GP method provides the most precise constraint on Ω_k, with a constraint precision of $\xi(\Omega_k) = 0.13$, surpassing recent estimations using similar methods. The GP method consistently indicates a preference for a flat universe at the 2σ confidence level. Moreover, we find that the choice of reconstruction method influences the estimation of Ω_k. The ANN reconstruction method exhibits higher sensitivity to the addition of BAO $H(z)$ data, resulting in comparable constraint precision to the GP method. A discrepancy exists between the best-fit values obtained by these two reconstruction methods, indicating their dependence on the reconstruction approach. However, we anticipate that with the improvement of sample size and precision of observational $H(z)$ data, the estimation of Ω_k using this approach will become more robust and reliable.

DOI: 10.1103/PhysRevD.108.063522

I. INTRODUCTION

After nearly a century of cosmological research, a standard cosmological model, the Λ cold dark matter (ΛCDM) model with six base parameters, was established, whose validity has been verified by almost all current observational data [1–5], especially by the *Planck*-satellite data with breathtaking precision [6,7]. However, as the precision of the observational data increases, some anomalies among different measurements of some key cosmological parameters are shaking our confidence in the standard cosmological model [7–14]. The most compelling ones appear to be the tension of the Hubble constant H_0 between the value inferred from the *Planck*-satellite data and the one inferred from the nearby type Ia supernovae (SNe Ia) data calibrated by the distance ladder, which has become a serious crisis for cosmology [15–28]. As far as the second anomaly is concerned, the S_8 parameter, a combination of the amplitude of matter density fluctuations and the matter density, is significantly lower in recent cosmic shear surveys than that expected according to the *Planck* data best fit ΛCDM model [29].

In addition, recently, an enhanced lensing amplitude in cosmic microwave background (CMB) power spectra from *Planck* 2018 data also presents another serious challenge to the standard cosmological model [7,12,14]. This effect could be explained naturally by a closed universe. However, the prevailing and very successful inflationary theory predicts a flat universe, and the observations also support a flat universe. For instance, the combination of CMB power spectra data and baryon acoustic oscillation (BAO) data puts a stringent constraint on the cosmic curvature parameter Ω_k under ΛCDM, strongly supporting a flat universe [3,6,7,30]. As a result, most cosmological research has long assumed a flat universe. However, the discovery of a closed universe at more than 3.4σ confidence level, preferred by the enhanced lensing amplitude in *Planck* 2018 data, suggests that this assumption may not be taken for granted [12,14]. What is worse is that the H_0 and S_8 tensions will be exacerbated when the possibility of a closed universe is considered, implying there may be even larger discordances hidden behind the assumption of a flat universe [12,13]. For a

*Corresponding author: zhangxin@mail.neu.edu.cn

comprehensive and detailed discussion on this topic, we recommend the reader to refer to Refs. [30–46]

In fact, all of these crises arise from the measurement inconsistencies between the early and late universe, and point to the fact that the cracks have appeared in the standard ΛCDM model. It is time to reconfirm what we once knew for sure. In this paper, we aim to thoroughly investigate whether the spatial geometry of our universe is open, flat, or closed with a cosmological model-independent method. This is not only in response to the crisis mentioned above but also because the spatial curvature of the universe is a significant issue that is deeply relevant to many fundamental questions in modern cosmology, such as the evolution of the universe and the property of the dark energy. The spatial geometry of the universe is usually described by the cosmic curvature parameter Ω_k, i.e., $\Omega_k > 0$, $\Omega_k = 0$, and $\Omega_k < 0$ correspond to an open, flat, and closed universe, respectively. In order to tackle the crisis arising from the measurements of cosmic curvature, a necessary approach is to use a cosmological model-independent method to confirm the value of Ω_k in the late universe. Recently, great progress has been made in this regard.

So far, many cosmological model-independent methods have been proposed to determine the cosmic curvature parameter Ω_k [9,47–54], in which a popular and effective method is applying the distance sum rule in the combination of strong gravitational lensing (SGL) and SNe Ia observations to constrain Ω_k [55]. Subsequently, this method has been fully implemented with the combination of SGL and other distance indicators, such as intermediate luminosity quasars and gravitational waves [9–11,56]. However, while it is true that this method is independent of cosmological models, Qi *et al.* [57] found that it is dependent on the mass distribution model of lens galaxies and is also affected by the classification of SGL data according to the lens velocity dispersion. To obtain an unbiased and precise estimate Ω_k in this way, it is crucial to accurately characterize the mass distribution of lens galaxies for each SGL sample, but this is still a long way off.

Another popular model-independent method to determine Ω_k is originally proposed to test the homogeneous and isotropic Friedmann-Lemaître-Robertson-Walker (FLRW) metric [51]. This method is derived from the theoretical expression between cosmological distance and the Hubble parameter $H(z)$, in which the cosmic curvature is involved. In reverse, the cosmic curvature could be estimated under the assumption of the FLRW metric. Subsequently, this estimation of Ω_k is implemented in several works in the light of new data and different statistical methods [58–60]. In most of these works, the Gaussian process, a nonparametric reconstruction technique, is widely used to reconstruct a smooth curve of $H(z)$ so that the distance at any redshift can be calibrated. Recently, Wang *et al.* [48,49] presented an alternative nonparametric approach based on the artificial neural network (ANN) for reconstructing a function from observational data, which also has been used in cosmological research, including the estimation of Ω_k.

In view of the importance of the cosmic curvature and the advances in sample size and precision of observational data, this paper aims to thoroughly investigate the extent to which the cosmic curvature parameter can be constrained in the late-universe by using the available observational data and various reconstruction techniques. We will employ the latest Pantheon + compilation of SNe Ia containing 1701 SNe Ia light curves and $60H(z)$ data obtained by two different observation methods to constrain the cosmic curvature parameter with two nonparametric approaches, GP and ANN.

II. DATA AND METHODOLOGY

We dedicate this section to describing the methodology and two observational datasets used in this paper.

A. Data: SNe Ia sample

We use the SNe Ia Pantheon + compilation containing 1701 light curves of 1550 unique in redshift range $0.001 < z < 2.26$ [61]. Compared to the original Pantheon compilation [62], the sample size of Pantheon + compilation has greatly increased, and the treatments of systematic uncertainties in redshifts, peculiar velocities, photometric calibration, and intrinsic scatter model of SNe Ia also have been improved. It should be noted that not all the SNe Ia in the Pantheon are included in the Pantheon + compilation.

In this paper, we make use of two different SNe Ia samples. Since the sensitivity of peculiar velocities is very large at low redshift ($z < 0.008$) as shown in Fig. 4 of Ref. [61], which may lead to biased results, we adopt the processing treatments used by Ref. [61], namely, remove the data points in redshift range $z < 0.01$. For convenience, we still call this dataset as Pantheon+. In addition, the Pantheon + dataset compiled by Ref. [61] also includes the recent Cepheid host distance anchors released by SH0ES (SNe, H0, for the equation of state of dark energy) Collaboration that facilitates constraints on both the standardized absolute magnitude of the SNe Ia M and H_0. Here, we also use this SNe Ia dataset and call it as Pantheon + &SH0ES.

While it is true that, in principle, the combination of $H(z)$ data with SNe Ia data can provide constraints on Ω_k, the inclusion of the SH0ES Cepheid calibration plays a crucial role in our analysis for several reasons. First, the determination of H_0 is highly sensitive to the constraint on Ω_k in our analysis. By combining the SH0ES Cepheid calibration, we benefit from an independent and remarkably precise measurement of H_0, which significantly enhances the accuracy of determining Ω_k. Second, the SH0ES Cepheid data allow for the calibration of the absolute magnitude of SNe Ia, providing a valuable anchor for cosmological distance measurements. This calibration is instrumental in achieving more reliable distance estimates. Finally, the synergy achieved by combining multiple

independent probes, such as the SH0ES Cepheid data, $H(z)$, and SNe Ia, facilitates a more robust and comprehensive determination of Ω_k, minimizing potential biases and yielding more confident results.

For each SN Ia, the observed distance module is given by

$$\mu_{\rm SN} = m_B - M_B, \tag{1}$$

where m_B is the observed magnitude in the rest-frame B-band. The theoretical distance modulus $\mu_{\rm th}$ is defined as

$$\mu_{\rm th} = 5\log_{10}\left[\frac{D_L(z)}{\rm Mpc}\right] + 25, \tag{2}$$

where $D_L(z)$ is the luminosity distance associated with the cosmological parameters. Constraining cosmological parameters is implemented by minimizing the χ^2 function:

$$-2\ \ln(\mathcal{L}) = \chi^2 = \Delta D^T \mathbf{C}^{-1}_{\rm stat+syst}\Delta D, \tag{3}$$

where D is the SNe Ia distance-modulus residuals computed as

$$\Delta D = \mu_{\rm SN} - \mu_{\rm th}, \tag{4}$$

and $\mathbf{C}_{\rm stat+syst}$ is the covariance matrix including both statistical and systematic errors, which could be found in the website,[1] as well as the SH0ES Cepheid host-distance covariance matrix.

B. Data: Hubble parameter measurements

The Hubble parameter $H(z)$ describes the expansion rate of the universe, and its observation is an important probe for exploring dark energy and the evolution of the universe. In general, there are two ways to measure $H(z)$. One is obtained by calculating the differential ages of galaxies, which is called cosmic chronometer (CC). We denote this $H(z)$ data obtained by this method as CC $H(z)$ [63–68]. Another is inferred from the baryon acoustic oscillation (BAO) peak in the galaxy's power spectrum. For convenience, we call this $H(z)$ as BAO $H(z)$ [69–80]. We have compiled the latest 32 CC $H(z)$ data points in Table I and 28 BAO $H(z)$ data points in Table II. In this paper, we preferentially use CC $H(z)$ data to constrain Ω_k, and then employ the total $H(z)$ data [CC $H(z)$+ BAO $H(z)$]. Considering the importance of properly accounting for the correlations between data points, in our analysis, we use the publicly available CC covariance tool[2] to estimate the covariance matrix for the CC data [65,66,68,81]. This allows us to appropriately incorporate the correlations and uncertainties associated with the CC measurements into our analysis. Furthermore, we have reanalyzed the results by considering the updated CC covariance and have found consistent results, reinforcing the robustness of our findings. The covariance matrix of the CC data is computed as

$$\mathbf{Cov}_{ij} = \mathbf{Cov}^{\rm stat}_{ij} + \mathbf{Cov}^{\rm sys}_{ij}, \tag{5}$$

where $\mathbf{Cov}^{\rm stat}_{ij}$ is the statistical errors. The systematic uncertainties $\mathbf{Cov}^{\rm sys}_{ij}$ encompass various effects associated with the determination of physical properties of galaxies, such as stellar metallicity and potential contamination from a young component. These effects are uncorrelated for objects at different redshifts. For a more comprehensive understanding of the origin and modeling of systematic errors in the CC data, we refer readers to Ref. [81].

TABLE I. The CC Hubble parameter $H(z)$ measurements and their errors $\sigma_{H(z)}$ at redshift z obtained from the differential age method.

Index	z	$H(z)$ [Mpc]	$\sigma_{H(z)}$ [Mpc]	Reference
1	0.07	69.0	19.6	[63]
2	0.1	69.0	12.0	[64]
3	0.12	68.6	26.2	[63]
4	0.17	83.0	8.0	[64]
5	0.1797	81.0	5.0	[65]
6	0.1993	81.0	6.0	[65]
7	0.2	72.9	29.6	[63]
8	0.27	77.0	14.0	[64]
9	0.28	88.8	36.6	[63]
10	0.3519	88.0	16.0	[65]
11	0.3802	89.2	14.1	[66]
12	0.4	95.0	17.0	[64]
13	0.4004	82.8	10.6	[66]
14	0.4247	93.7	11.7	[66]
15	0.4293	91.8	5.3	[66]
16	0.4497	99.7	13.4	[66]
17	0.47	89.0	49.65	[67]
18	0.4783	80.9	9.0	[66]
19	0.48	97.0	60.0	[64]
20	0.5929	110.0	15.0	[65]
21	0.6797	98.0	10.0	[65]
22	0.7812	88.0	11.0	[65]
23	0.8754	124.0	17.0	[65]
24	0.88	90.0	40.0	[64]
25	0.9	117.0	23.0	[64]
26	1.037	113.0	15.0	[65]
27	1.3	168.0	17.0	[64]
28	1.363	160.0	33.6	[68]
29	1.43	177.0	18.0	[64]
30	1.53	140.0	14.0	[64]
31	1.75	202.0	40.0	[64]
32	1.965	186.5	50.4	[68]

C. Reconstruction method: Gaussian process

There is an integral between the Hubble parameter and the luminosity distance. In order to calibrate the distance

[1] https://github.com/PantheonPlusSH0ES/DataRelease.
[2] https://gitlab.com/mmoresco/CCcovariance.

TABLE II. The BAO Hubble parameter measurements $H(z)$ and their errors $\sigma_{H(z)}$ at redshift z obtained from the radial BAO method.

Index	z	$H(z)$ [Mpc]	$\sigma_{H(z)}$ [Mpc]	Reference
1	0.24	79.69	2.99	[69]
2	0.3	81.7	6.22	[70]
3	0.31	78.17	4.74	[71]
4	0.34	83.80	3.66	[69]
5	0.35	82.70	8.40	[72]
6	0.36	79.93	3.39	[71]
7	0.38	81.50	1.90	[73]
8	0.40	82.04	2.03	[71]
9	0.43	86.45	3.68	[69]
10	0.44	84.81	1.83	[71]
11	0.48	87.79	2.03	[71]
12	0.51	90.40	1.90	[73]
13	0.52	94.35	2.65	[71]
14	0.56	93.33	2.32	[71]
15	0.57	96.80	3.40	[74]
16	0.59	98.48	3.19	[71]
17	0.6	87.90	6.10	[75]
18	0.61	97.30	2.10	[73]
19	0.64	98.82	2.99	[71]
20	0.73	97.30	7.00	[75]
21	0.978	113.72	14.63	[76]
22	1.23	131.44	12.42	[76]
23	1.526	148.11	12.71	[76]
24	1.944	172.63	14.79	[76]
25	2.3	224.00	8.00	[77]
26	2.33	224.00	8.00	[78]
27	2.34	222.00	7.00	[79]
28	2.36	226.00	8.00	[80]

using the $H(z)$ data, it is necessary to reconstruct a smooth curve of $H(z)$ with a nonparametric reconstruction technique firstly. Here, we briefly introduce the GP method that allows us to reconstruct a function from data straightforwardly without any parametric assumption. We adopt the GAPP Python code widely used in cosmology to implement the GP method [48,82–90]. In this process, it is assumed that the value of the reconstructed function $f(z)$ evaluated at two different points z and $\tilde{z}$ are connected by a covariance function $k(z,\tilde{z})$, and it only depends on two hyperparameters σ_f and ℓ. Although there are various and effective forms of the covariance function, according to the analysis in Seikel and Clarkson [86], the squared exponential form with the Matérn ($\nu = 9/2$) covariance function can lead to more reliable results than all others. So we take it here, and its expression is

$$k(z,\tilde{z}) = \sigma_f^2 \exp\left(-\frac{3|z-\tilde{z}|}{\ell}\right)\left(1+\frac{3|z-\tilde{z}|}{\ell}+\frac{27(z-\tilde{z})^2}{7\ell^2} + \frac{18|z-\tilde{z}|^3}{7\ell^3}+\frac{27(z-\tilde{z})^4}{35\ell^4}\right). \quad (6)$$

Here, the hyperparameter ℓ represents the characteristic length scale, indicating the distance over which significant changes occur in the function $f(z)$. The hyperparameter σ_f represents the typical change or variation in the observed data. The values of two hyperparameters are optimized by the GP itself via the observational data. It is important to note that the optimization of these two hyperparameters is performed independently of the fitting process for the cosmological parameters. The reconstructed functions of $H(z)$ for the two cases, CC $H(z)$ and total $H(z)$, are shown in Fig. 1.

D. Reconstruction method: artificial neural network

Here, we use the ANN method based on REFANN [49] Python code to reconstruct a function of $H(z)$ from data, which also has been widely used in cosmology [87,91].

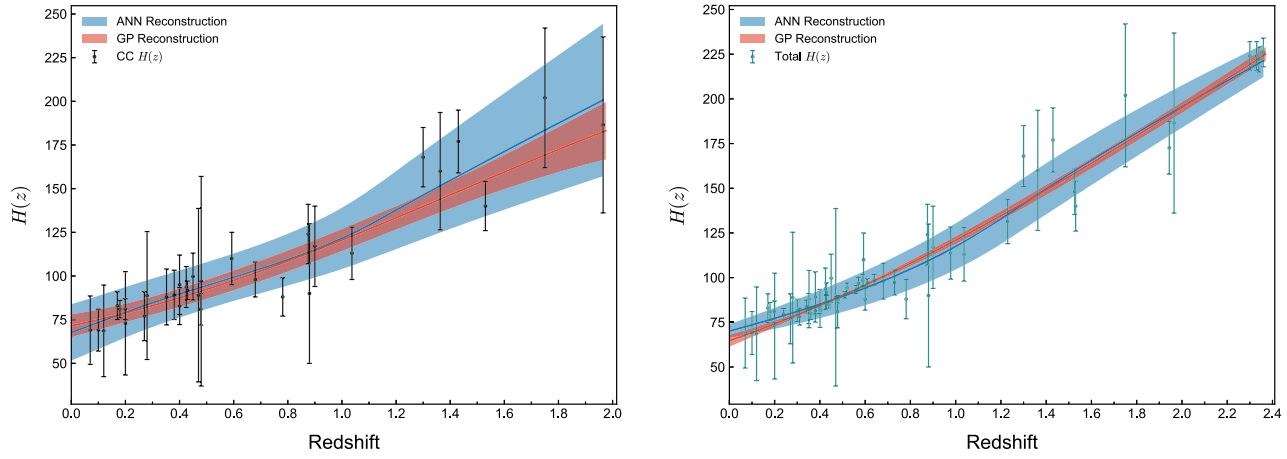

FIG. 1. Left: The reconstructions of $H(z)$ from CC $H(z)$ data by using GP (red region) and ANN (blue region). The shaded region and the solid line denote the 1σ confidence level errors and the best-fit values of reconstruction, respectively. The black points with error bars represent the observed CC $H(z)$ data. Right: Same as the left panel but for the total $H(z)$ data.

The ANN method, completely driven by data, allows us to reconstruct a function from any kind of data without assuming a parametrization of the function. The optimal ANN model of reconstructing functions we used is the same as that selected by Wang *et al.* [49], which has one hidden layer with 4096 neurons total. The reconstructed functions of $H(z)$ from the ANN are also shown in Fig. 1.

We can see that the confidence region reconstructed from the ANN is larger than that reconstructed from the GP method, which may be due to the basic logic and nature of these two techniques. One potential explanation for the observed discrepancy is the variance in the underlying assumptions and modeling approaches of GP and ANN. The GP method focuses on reconstructing a smooth function based on the covariance between data points, prioritizing the overall structure and correlations in the data. On the other hand, ANN approximates the underlying function using interconnected artificial neurons, allowing it to capture complex nonlinear relationships. These inherent differences in modeling techniques can lead to variations in how the methods handle noise, outliers, and subtle features in the data, resulting in divergent reconstructions for $H(z)$. Additionally, the training and optimization processes employed by GP and ANN can contribute to the observed discrepancy. The selection of hyperparameters, such as the kernel function in GP or the network architecture in ANN, can significantly impact the models' flexibility and generalization capabilities. Variations in the hyperparameter selection and training strategies may introduce sensitivities and biases that influence the inferred values of $H(z)$. Furthermore, it is important to acknowledge that GP and ANN have distinct strengths and limitations. GP excels at capturing uncertainties and estimating smooth functions, while ANN is effective in modeling complex nonlinear relationships. These inherent differences in methodology can contribute to the observed discrepancies in the reconstructed values of $H(z)$.

In addition, the reconstructed values of Hubble constant $[H(z=0)]$ by these two methods are also different, which is sensitive to the constraint on Ω_k as we will see later.

E. Methodology for estimation of Ω_k

In the framework of the FLRW metric, the comoving distance $D_C(z)$ is defined as

$$D_C(z) = c\int_0^z \frac{dz'}{H(z')}, \tag{7}$$

where c is the speed of light. With a reconstructed smooth function of $H(z)$, a smooth function of $D_C(z)$ could be calculated by integrating the function $H(z)$, and its confidence region also could be obtained by integrating the error of $H(z)$. Furthermore, the luminosity distance D_L could be obtained by D_C via

$$\frac{D_L}{(1+z)} = \begin{cases} \frac{c}{H_0}\frac{1}{\sqrt{\Omega_k}}\sinh\left[\sqrt{\Omega_k}D_C\frac{H_0}{c}\right] & \Omega_k > 0, \\ D_C & \Omega_k = 0, \\ \frac{c}{H_0}\frac{1}{\sqrt{|\Omega_k|}}\sin\left[\sqrt{|\Omega_k|}D_C\frac{H_0}{c}\right] & \Omega_k < 0. \end{cases} \tag{8}$$

Note that in this calculation, the value of H_0 is adopted from the reconstructed value of $H(z=0)$. The uncertainty of D_L could be obtained by

$$\sigma_{D_L} = \begin{cases} (1+z)\cosh\left[\sqrt{|\Omega_k|}D_C\frac{H_0}{c}\right]\sigma_{D_C} & \text{for } \Omega_k > 0, \\ (1+z)\sigma_{D_C} & \text{for } \Omega_k = 0, \\ (1+z)\cos\left[\sqrt{|\Omega_k|}D_C\frac{H_0}{c}\right]\sigma_{D_C} & \text{for } \Omega_k < 0. \end{cases} \tag{9}$$

The distance modulus reconstructed from $H(z)$ data μ_H can be further obtained by Eq. (2). Finally, the cosmic curvature parameter Ω_k could be estimated by minimizing the χ^2 function of Eq. (3). Here, the uncertainty of reconstructed distance modulus σ_{μ_H} should be added to the covariance matrix as a systematic error via

$$(\mathbf{C}_{\rm stat})_{ii} = (\mathbf{C}^{\rm SN}_{\rm stat})_{ii} + \sigma^2_{\mu_H,i}. \tag{10}$$

We constrain the cosmological parameters using the EMCEE Python module based on the Markov Chain Monte Carlo analysis [92]. There are two free parameters, Ω_k and the SNe Ia absolute magnitude M_B.

III. RESULTS AND DISCUSSIONS

Here, we combine two types of $H(z)$ data, two types of SNe Ia data, and two reconstruction methods to make a thorough investigation of the cosmic curvature. All the constraint contours of Ω_k and M_B are shown in Figs. 2–3 and the best-fit values with 1σ confidence level are listed in Table III.

In Fig. 2, we present the constraints on Ω_k and M_B obtained from the CC $H(z)$ data in different scenarios. It is evident that there are differences between the contours derived from the two reconstruction methods. Specifically, concerning the GP method, the values of M_B constrained from both the Pantheon+ and Pantheon + &SH0ES datasets are almost identical, which means the addition of SH0ES data is not helpful to the constraint on M_B. As for Ω_k, the estimations from Pantheon+ and Pantheon + &SH0ES both favor a closed universe, while remaining consistent with a flat universe at the 2σ confidence level. Moreover, we find an intriguing finding that the inclusion of SH0ES data does not appear to significantly impact the precision of the Ω_k constraint.

Regarding the ANN method, we find that the uncertainties of the two parameters (i.e., Ω_k and M_B) obtained from

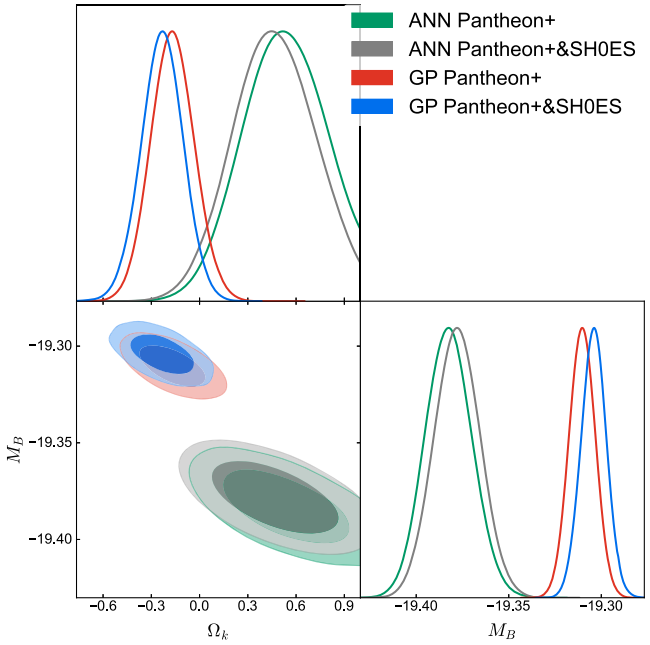

FIG. 2. The constraints with the 1σ and 2σ confidence level on the cosmic curvature Ω_k and the SNe Ia absolute magnitude M_B from two types of SNe Ia dataset (Pantheon+ and Pantheon + &SH0ES) and with two reconstruction methods (GP and ANN), respectively, in the case of CC $H(z)$ data.

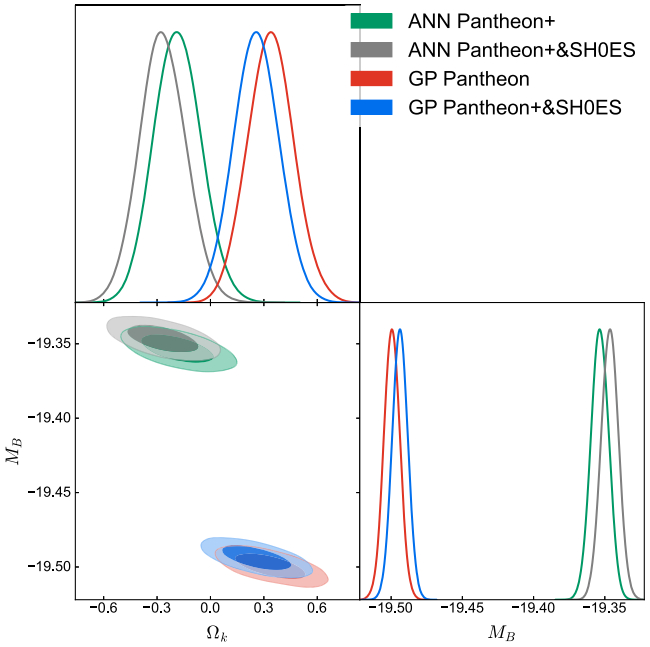

FIG. 3. Same as Fig. 2, but for Total $H(z)$ data.

this approach are larger than those derived from the GP method. This discrepancy can be traced back to the left panel of Fig. 1, where we notice that the confidence region of $H(z)$ reconstructed by the ANN is notably broader compared to that reconstructed using the GP method. Additionally, as mentioned previously, the reconstructed values of the Hubble constant $[H(z=0)]$ from these two methods are also different, which subsequently influences the constraint on M_B as evident from the distinct contours observed in Fig. 2 for the GP and ANN methods. Concerning the estimation of Ω_k, we find that not only do the uncertainties become larger when compared to the results obtained from the GP method, but the best-fit values also tend to favor an open universe, while remaining consistent with a flat universe within the 2σ confidence level. Additionally, the addition of SH0ES data does not appear to significantly affect the constraint precision of Ω_k in the context of the ANN method.

Now, let's focus on the Total $H(z)$ data, which has a sample size nearly twice as large as the CC $H(z)$ data. In Fig. 3, we present the 1D and 2D marginalized probability distributions of Ω_k and M_B obtained from this dataset.

For the GP method, regarding the constraints on Ω_k, we find a shift in the best-fit values compared with CC $H(z)$ data, now leaning toward a positive value, indicating support for an open universe, but the estimate from Pantheon + &SH0ES is still consistent with a flat universe at 2σ confidence level. This change demonstrates that the addition of the BAO $H(z)$ observational data influences the estimation of Ω_k using this approach. Despite the total $H(z)$ data having nearly twice the sample size of the CC $H(z)$ data, we find that the constraint precision of Ω_k is not notably improved compared to that derived from the CC $H(z)$ data.

In the case of the ANN reconstruction method, we find a substantial improvement in the constraints on both Ω_k and M_B when using the total $H(z)$ data compared to the results obtained from the CC $H(z)$ data. The constraints on Ω_k and M_B have improved by approximately twice, indicating that the ANN method is more sensitive to the addition of the BAO $H(z)$ data. This sensitivity allows for better constraints on the cosmological parameters when incorporating the larger sample size provided by the Total $H(z)$ data. Regarding Ω_k, both of the best-fit values from the two

TABLE III. The constraint results of Ω_k and M_B with 1σ confidence level for various datasets and reconstruction methods.

$H(z)$ data type	Parameters	GP Pantheon+	GP Pantheon + &SH0ES	ANN Pantheon+	ANN Pantheon + &SH0ES
CC $H(z)$	Ω_k	-0.17 ± 0.13	-0.23 ± 0.13	$0.51^{+0.27}_{-0.24}$	0.46 ± 0.25
	M_B	-19.310 ± 0.007	-19.304 ± 0.007	-19.382 ± 0.013	-19.378 ± 0.012
Total $H(z)$	Ω_k	0.34 ± 0.13	0.26 ± 0.13	-0.18 ± 0.13	-0.27 ± 0.13
	M_B	-19.500 ± 0.006	-19.494 ± 0.005	-19.353 ± 0.006	-19.3465 ± 0.006

SNe Ia datasets favor a closed universe, while remaining consistent with a flat universe within the 2σ confidence level.

IV. CONCLUSION

Currently, the measurement inconsistencies between the early and late universe, such as the tensions in the Hubble constant, the S_8 parameter, and the cosmic curvature parameter, have raised questions about the validity of the standard cosmological model, i.e., the ΛCDM model. In this paper, we highlight the importance of determining the cosmic curvature parameter Ω_k and aim to make a thorough investigation for the model-independent measurement of Ω_k in the late universe with the observational data and statistical tools available to us. Therefore, we consider two types of $H(z)$ datasets (CC $H(z)$ data and total data), two types of SNe Ia datasets (Pantheon+ and Pantheon + &SH0ES), and two reconstruction methods (GP method and ANN method).

The GP method has yielded the most precise constraint on Ω_k, with a constraint precision of $\xi(\Omega_k) = 0.13$ for any combination of data, surpassing the recent measurements of Ω_k using similar methods [48,58–60]. Overall, the estimations obtained through the GP method consistently support a flat universe at the 2σ confidence level.

It is worth noting that the estimation of Ω_k in this study is influenced by the choice of reconstruction method. The ANN reconstruction method exhibits higher sensitivity to the addition of $H(z)$ data. By combining the BAO $H(z)$ data, the constraint precision based on the ANN method becomes comparable to that obtained using the GP method. However, a discrepancy exists between the best-fit values obtained by these two reconstruction methods, indicating a dependence on the reconstruction approach. As a consequence, the method employed in this study to evaluate Ω_k may be less robust due to its sensitivity to the reconstruction method. Nevertheless, we expect that with the improvement of sample size and precision of observational $H(z)$ data, the estimation of Ω_k using this approach will become more robust and reliable.

ACKNOWLEDGMENTS

This work was supported by the National SKA Program of China (Grants Nos. 2022SKA0110200 and 2022SKA0110203), and the National Natural Science Foundation of China (Grants Nos. 12205039, 11975072, 11835009, and 11875102).

[1] Adam G. Riess *et al.* (Supernova Search Team Collaboration), Observational evidence from supernovae for an accelerating universe and a cosmological constant, Astron. J. **116**, 1009 (1998).
[2] S. Perlmutter *et al.* (Supernova Cosmology Project Collaboration), Measurements of Ω and Λ from 42 high redshift supernovae, Astrophys. J. **517**, 565 (1999).
[3] D. N. Spergel *et al.* (WMAP Collaboration), First year Wilkinson Microwave Anisotropy Probe (WMAP) observations: Determination of cosmological parameters, Astrophys. J. Suppl. Ser. **148**, 175 (2003).
[4] Max Tegmark *et al.* (SDSS Collaboration), Cosmological parameters from SDSS and WMAP, Phys. Rev. D **69**, 103501 (2004).
[5] Kevork Abazajian *et al.* (SDSS Collaboration), The second data release of the Sloan digital sky survey, Astron. J. **128**, 502 (2004).
[6] P. A. R. Ade *et al.* (Planck Collaboration), Planck 2015 results. XIII. Cosmological parameters, Astron. Astrophys. **594**, A13 (2016).
[7] N. Aghanim *et al.* (Planck Collaboration), Planck 2018 results. VI. Cosmological parameters, Astron. Astrophys. **641**, A6 (2020); **652**, C4(E) (2021).
[8] Adam G. Riess, Stefano Casertano, Wenlong Yuan, Lucas M. Macri, and Dan Scolnic, Large magellanic cloud Cepheid standards provide a 1% foundation for the determination of the Hubble constant and stronger evidence for physics beyond ΛCDM, Astrophys. J. **876**, 85 (2019).
[9] Jing-Zhao Qi, Jia-Wei Zhao, Shuo Cao, Marek Biesiada, and Yuting Liu, Measurements of the Hubble constant and cosmic curvature with quasars: Ultracompact radio structure and strong gravitational lensing, Mon. Not. R. Astron. Soc. **503**, 2179 (2021).
[10] Jing-Zhao Qi, Yu Cui, Wei-Hong Hu, Jing-Fei Zhang, Jing-Lei Cui, and Xin Zhang, Strongly lensed type Ia supernovae as a precise late-Universe probe of measuring the Hubble constant and cosmic curvature, Phys. Rev. D **106**, 023520 (2022).
[11] Meng-Di Cao, Jie Zheng, Jing-Zhao Qi, Xin Zhang, and Zong-Hong Zhu, A new way to explore cosmological tensions using gravitational waves and strong gravitational lensing, Astrophys. J. **934**, 108 (2022).
[12] Eleonora Di Valentino, Alessandro Melchiorri, and Joseph Silk, Planck evidence for a closed universe and a possible crisis for cosmology, Nat. Astron. **4**, 196 (2019).
[13] Eleonora Di Valentino, Alessandro Melchiorri, and Joseph Silk, Investigating cosmic discordance, Astrophys. J. Lett. **908**, L9 (2021).
[14] Will Handley, Curvature tension: Evidence for a closed universe, Phys. Rev. D **103**, L041301 (2021).
[15] Adam G. Riess, Stefano Casertano, Wenlong Yuan, J. Bradley Bowers, Lucas Macri, Joel C. Zinn, and Dan Scolnic, Cosmic distances calibrated to 1% precision with

Gaia EDR3 parallaxes and Hubble space telescope photometry of 75 milky way cepheids confirm tension with ΛCDM, Astrophys. J. Lett. **908**, L6 (2021).
[16] Eleonora Di Valentino, Olga Mena, Supriya Pan, Luca Visinelli, Weiqiang Yang, Alessandro Melchiorri, David F. Mota, Adam G. Riess, and Joseph Silk, In the realm of the Hubble tension—a review of solutions, Classical Quantum Gravity **38**, 153001 (2021).
[17] Sunny Vagnozzi, New physics in light of the H_0 tension: An alternative view, Phys. Rev. D **102**, 023518 (2020).
[18] Xin Zhang, Gravitational wave standard sirens and cosmological parameter measurement, Sci. China Phys. Mech. Astron. **62**, 110431 (2019).
[19] YiDong Xu and Xin Zhang, Cosmological parameter measurement and neutral hydrogen 21 cm sky survey with the Square Kilometre Array, Sci. China Phys. Mech. Astron. **63**, 270431 (2020).
[20] Miao Li, Xiao-Dong Li, Yin-Zhe Ma, Xin Zhang, and Zhenhui Zhang, Planck constraints on holographic dark energy, J. Cosmol. Astropart. Phys. 09 (2013) 021.
[21] Jing-Zhao Qi and Xin Zhang, A new cosmological probe using super-massive black hole shadows, Chin. Phys. C **44**, 055101 (2020).
[22] Kyriakos Vattis, Savvas M. Koushiappas, and Abraham Loeb, Dark matter decaying in the late universe can relieve the H0 tension, Phys. Rev. D **99**, 121302 (2019).
[23] Jing-Fei Zhang, Jia-Jia Geng, and Xin Zhang, Neutrinos and dark energy after Planck and BICEP2: Data consistency tests and cosmological parameter constraints, J. Cosmol. Astropart. Phys. 10 (2014) 044.
[24] Rui-Yun Guo, Jing-Fei Zhang, and Xin Zhang, Can the H_0 tension be resolved in extensions to ΛCDM cosmology? J. Cosmol. Astropart. Phys. 02 (2019) 054.
[25] Ming-Ming Zhao, Dong-Ze He, Jing-Fei Zhang, and Xin Zhang, Search for sterile neutrinos in holographic dark energy cosmology: Reconciling Planck observation with the local measurement of the Hubble constant, Phys. Rev. D **96**, 043520 (2017).
[26] Rui-Yun Guo and Xin Zhang, Constraints on inflation revisited: An analysis including the latest local measurement of the Hubble constant, Eur. Phys. J. C **77**, 882 (2017).
[27] Li-Yang Gao, Ze-Wei Zhao, She-Sheng Xue, and Xin Zhang, Relieving the H 0 tension with a new interacting dark energy model, J. Cosmol. Astropart. Phys. 07 (2021) 005.
[28] Li-Yang Gao, She-Sheng Xue, and Xin Zhang, Dark energy and matter interacting scenario can relieve H_0 and S_8 tensions, arXiv:2212.13146.
[29] Catherine Heymans *et al.*, KiDS-1000 Cosmology: Multi-probe weak gravitational lensing and spectroscopic galaxy clustering constraints, Astron. Astrophys. **646**, A140 (2021).
[30] Jordan Stevens, Hasti Khoraminezhad, and Shun Saito, Constraining the spatial curvature with cosmic expansion history in a cosmological model with a nonstandard sound horizon, J. Cosmol. Astropart. Phys. 07 (2023) 046.
[31] George Efstathiou and Steven Gratton, The evidence for a spatially flat universe, Mon. Not. R. Astron. Soc. **496**, L91 (2020).
[32] Sunny Vagnozzi, Eleonora Di Valentino, Stefano Gariazzo, Alessandro Melchiorri, Olga Mena, and Joseph Silk, The galaxy power spectrum take on spatial curvature and cosmic concordance, Phys. Dark Universe **33**, 100851 (2021).
[33] Sunny Vagnozzi, Abraham Loeb, and Michele Moresco, Eppur è piatto? The cosmic chronometers take on spatial curvature and cosmic concordance, Astrophys. J. **908**, 84 (2021).
[34] Javier E. Gonzalez, Micol Benetti, Rodrigo von Marttens, and Jailson Alcaniz, Testing the consistency between cosmological data: The impact of spatial curvature and the dark energy EoS, J. Cosmol. Astropart. Phys. 11 (2021) 060.
[35] Ella Zuckerman and Luis A. Anchordoqui, Spatial curvature sensitivity to local H0 from the Cepheid distance ladder, J. High Energy Astrophys. **33**, 10 (2022).
[36] Ozgur Akarsu, Eleonora Di Valentino, Suresh Kumar, Maya Ozyigit, and Shivani Sharma, Testing spatial curvature and anisotropic expansion on top of the ΛCDM model, Phys. Dark Universe **39**, 101162 (2023).
[37] Aaron Glanville, Cullan Howlett, and Tamara M. Davis, Full-shape galaxy power spectra and the curvature tension, Mon. Not. R. Astron. Soc. **517**, 3087 (2022).
[38] Julien Bel, Julien Larena, Roy Maartens, Christian Marinoni, and Louis Perenon, Constraining spatial curvature with large-scale structure, J. Cosmol. Astropart. Phys. 09 (2022) 076.
[39] Arianna Favale, Adrià Gómez-Valent, and Marina Migliaccio, Cosmic chronometers to calibrate the ladders and measure the curvature of the universe. A model-independent study, Mon. Not. R. Astron. Soc. **523**, 3406 (2023).
[40] Shulei Cao, Joseph Ryan, and Bharat Ratra, Using Pantheon and DES supernova, baryon acoustic oscillation, and Hubble parameter data to constrain the Hubble constant, dark energy dynamics, and spatial curvature, Mon. Not. R. Astron. Soc. **504**, 300 (2021).
[41] Zhongxu Zhai, Chan-Gyung Park, Yun Wang, and Bharat Ratra, CMB distance priors revisited: Effects of dark energy dynamics, spatial curvature, primordial power spectrum, and neutrino parameters, J. Cosmol. Astropart. Phys. 07 (2020) 009.
[42] Joseph Ryan, Yun Chen, and Bharat Ratra, Baryon acoustic oscillation, Hubble parameter, and angular size measurement constraints on the Hubble constant, dark energy dynamics, and spatial curvature, Mon. Not. R. Astron. Soc. **488**, 3844 (2019).
[43] Chan-Gyung Park and Bharat Ratra, Measuring the Hubble constant and spatial curvature from supernova apparent magnitude, baryon acoustic oscillation, and Hubble parameter data, Astrophys. Space Sci. **364**, 134 (2019).
[44] Jarred Penton, Jacob Peyton, Aasim Zahoor, and Bharat Ratra, Median statistics analysis of deuterium abundance measurements and spatial curvature constraints, Publ. Astron. Soc. Pac. **130**, 114001 (2018).
[45] Joseph Ryan, Sanket Doshi, and Bharat Ratra, Constraints on dark energy dynamics and spatial curvature from Hubble parameter and baryon acoustic oscillation data, Mon. Not. R. Astron. Soc. **480**, 759 (2018).

[46] Hai Yu, Bharat Ratra, and Fa-Yin Wang, Hubble parameter and baryon acoustic oscillation measurement constraints on the Hubble constant, the deviation from the spatially flat ΛCDM model, the deceleration–acceleration transition redshift, and spatial curvature, Astrophys. J. **856**, 3 (2018).
[47] Thomas Collett, Francesco Montanari, and Syksy Rasanen, Model-Independent Determination of H_0 and Ω_{K0} from Strong Lensing and Type Ia Supernovae, Phys. Rev. Lett. **123**, 231101 (2019).
[48] Guo-Jian Wang, Xiao-Jiao Ma, and Jun-Qing Xia, Machine learning the cosmic curvature in a model-independent way, Mon. Not. R. Astron. Soc. **501**, 5714 (2021).
[49] Guo-Jian Wang, Xiao-Jiao Ma, Si-Yao Li, and Jun-Qing Xia, Reconstructing functions and estimating parameters with artificial neural networks: A test with a Hubble parameter and SNe Ia, Astrophys. J. Suppl. Ser. **246**, 13 (2020).
[50] Chris Clarkson, Marina Cortes, and Bruce A. Bassett, Dynamical dark energy or simply cosmic curvature?, J. Cosmol. Astropart. Phys. 08 (2007) 011.
[51] Chris Clarkson, Bruce Bassett, and Teresa Hui-Ching Lu, A General Test of the Copernican Principle, Phys. Rev. Lett. **101**, 011301 (2008).
[52] Bo Wang, Jing-Zhao Qi, Jing-Fei Zhang, and Xin Zhang, Cosmological model-independent constraints on spatial curvature from strong gravitational lensing and SN Ia observations, Astrophys. J. **898**, 100 (2020).
[53] Jun-Qing Xia, Hai Yu, Guo-Jian Wang, Shu-Xun Tian, Zheng-Xiang Li, Shuo Cao, and Zong-Hong Zhu, Revisiting studies of the statistical property of a strong gravitational lens system and model-independent constraint on the curvature of the universe, Astrophys. J. **834**, 75 (2017).
[54] Rong-Gen Cai, Zong-Kuan Guo, and Tao Yang, Null test of the cosmic curvature using $H(z)$ and supernovae data, Phys. Rev. D **93**, 043517 (2016).
[55] Syksy Räsänen, Krzysztof Bolejko, and Alexis Finoguenov, New Test of the Friedmann-Lemaître-Robertson-Walker Metric Using the Distance Sum Rule, Phys. Rev. Lett. **115**, 101301 (2015).
[56] Yan-Jin Wang, Jing-Zhao Qi, Bo Wang, Jing-Fei Zhang, Jing-Lei Cui, and Xin Zhang, Cosmological model-independent measurement of cosmic curvature using distance sum rule with the help of gravitational waves, Mon. Not. R. Astron. Soc. **516**, 5187 (2022).
[57] Jing-Zhao Qi, Shuo Cao, Sixuan Zhang, Marek Biesiada, Yan Wu, and Zong-Hong Zhu, The distance sum rule from strong lensing systems and quasars—test of cosmic curvature and beyond, Mon. Not. R. Astron. Soc. **483**, 1104 (2019).
[58] Jun-Jie Wei and Xue-Feng Wu, An improved method to measure the cosmic curvature, Astrophys. J. **838**, 160 (2017).
[59] H. Yu and F. Y. Wang, New model-independent method to test the curvature of the universe, Astrophys. J. **828**, 85 (2016).
[60] Suhail Dhawan, Justin Alsing, and Sunny Vagnozzi, Non-parametric spatial curvature inference using late-universe cosmological probes, Mon. Not. R. Astron. Soc. **506**, L1 (2021).
[61] Dillon Brout *et al.*, The Pantheon + Analysis: Cosmological constraints, Astrophys. J. **938**, 110 (2022).
[62] D. M. Scolnic *et al.* (Pan-STARRS1 Collaboration), The complete light-curve sample of spectroscopically confirmed SNe Ia from Pan-STARRS1 and cosmological constraints from the combined Pantheon sample, Astrophys. J. **859**, 101 (2018).
[63] Cong Zhang, Han Zhang, Shuo Yuan, Tong-Jie Zhang, and Yan-Chun Sun, Four new observational $H(z)$ data from luminous red galaxies in the Sloan Digital Sky Survey data release seven, Res. Astron. Astrophys. **14**, 1221 (2014).
[64] Daniel Stern, Raul Jimenez, Licia Verde, Marc Kamionkowski, and S. Adam Stanford, Cosmic chronometers: Constraining the equation of state of dark energy. I: H(z) Measurements, J. Cosmol. Astropart. Phys. 02 (2010) 008.
[65] M. Moresco *et al.*, Improved constraints on the expansion rate of the universe up to z˜1.1 from the spectroscopic evolution of cosmic chronometers, J. Cosmol. Astropart. Phys. 08 (2012) 006.
[66] Michele Moresco, Lucia Pozzetti, Andrea Cimatti, Raul Jimenez, Claudia Maraston, Licia Verde, Daniel Thomas, Annalisa Citro, Rita Tojeiro, and David Wilkinson, A 6% measurement of the Hubble parameter at $z \sim 0.45$: Direct evidence of the epoch of cosmic re-acceleration, J. Cosmol. Astropart. Phys. 05 (2016) 014.
[67] A. L. Ratsimbazafy, S. I. Loubser, S. M. Crawford, C. M. Cress, B. A. Bassett, R. C. Nichol, and P. Väisänen, Age-dating luminous red galaxies observed with the Southern African Large Telescope, Mon. Not. R. Astron. Soc. **467**, 3239 (2017).
[68] Michele Moresco, Raising the bar: New constraints on the Hubble parameter with cosmic chronometers at z ∼ 2, Mon. Not. R. Astron. Soc. **450**, L16 (2015).
[69] Enrique Gaztanaga, Anna Cabre, and Lam Hui, Clustering of luminous red galaxies IV: Baryon acoustic peak in the line-of-sight direction and a direct measurement of H(z), Mon. Not. R. Astron. Soc. **399**, 1663 (2009).
[70] Akira Oka, Shun Saito, Takahiro Nishimichi, Atsushi Taruya, and Kazuhiro Yamamoto, Simultaneous constraints on the growth of structure and cosmic expansion from the multipole power spectra of the SDSS DR7 LRG sample, Mon. Not. R. Astron. Soc. **439**, 2515 (2014).
[71] Yuting Wang *et al.* (BOSS Collaboration), The clustering of galaxies in the completed SDSS-III Baryon Oscillation Spectroscopic Survey: Tomographic BAO analysis of DR12 combined sample in configuration space, Mon. Not. R. Astron. Soc. **469**, 3762 (2017).
[72] Chia-Hsun Chuang and Yun Wang, Modeling the anisotropic two-point galaxy correlation function on small scales and improved measurements of $H(z)$, $D_A(z)$, and $\beta(z)$ from the Sloan digital sky survey DR7 luminous red galaxies, Mon. Not. R. Astron. Soc. **435**, 255 (2013).
[73] Shadab Alam *et al.* (BOSS Collaboration), The clustering of galaxies in the completed SDSS-III Baryon Oscillation Spectroscopic Survey: Cosmological analysis of the DR12 galaxy sample, Mon. Not. R. Astron. Soc. **470**, 2617 (2017).

[74] Lauren Anderson *et al.* (BOSS Collaboration), The clustering of galaxies in the SDSS-III Baryon Oscillation Spectroscopic Survey: Baryon acoustic oscillations in the data releases 10 and 11 galaxy samples, Mon. Not. R. Astron. Soc. **441**, 24 (2014).

[75] Chris Blake *et al.*, The WiggleZ Dark Energy Survey: Joint measurements of the expansion and growth history at z < 1, Mon. Not. R. Astron. Soc. **425**, 405 (2012).

[76] Gong-Bo Zhao *et al.*, The clustering of the SDSS-IV extended baryon oscillation spectroscopic survey DR14 quasar sample: A tomographic measurement of cosmic structure growth and expansion rate based on optimal redshift weights, Mon. Not. R. Astron. Soc. **482**, 3497 (2019).

[77] Nicolas G. Busca *et al.*, Baryon acoustic oscillations in the Ly-α forest of BOSS quasars, Astron. Astrophys. **552**, A96 (2013).

[78] Julian E. Bautista *et al.*, Measurement of baryon acoustic oscillation correlations at $z = 2.3$ with SDSS DR12 Lyα-Forests, Astron. Astrophys. **603**, A12 (2017).

[79] Timothée Delubac *et al.* (BOSS Collaboration), Baryon acoustic oscillations in the Lyα forest of BOSS DR11 quasars, Astron. Astrophys. **574**, A59 (2015).

[80] Andreu Font-Ribera *et al.* (BOSS Collaboration), Quasar-Lyman α forest cross-correlation from BOSS DR11: Baryon acoustic oscillations, J. Cosmol. Astropart. Phys. 05 (2014) 027.

[81] Michele Moresco, Raul Jimenez, Licia Verde, Andrea Cimatti, and Lucia Pozzetti, Setting the stage for cosmic chronometers. II. Impact of stellar population synthesis models systematics and full covariance matrix, Astrophys. J. **898**, 82 (2020).

[82] Marina Seikel, Chris Clarkson, and Mathew Smith, Reconstruction of dark energy and expansion dynamics using Gaussian processes, J. Cosmol. Astropart. Phys. 06 (2012) 036.

[83] Marina Seikel, Sahba Yahya, Roy Maartens, and Chris Clarkson, Using H(z) data as a probe of the concordance model, Phys. Rev. D **86**, 083001 (2012).

[84] Ming-Jian Zhang and Hong Li, Gaussian processes reconstruction of dark energy from observational data, Eur. Phys. J. C **78**, 460 (2018).

[85] Yi-Fu Cai, Martiros Khurshudyan, and Emmanuel N. Saridakis, Model-independent reconstruction of $f(T)$ gravity from Gaussian processes, Astrophys. J. **888**, 62 (2020).

[86] Marina Seikel and Chris Clarkson, Optimising Gaussian processes for reconstructing dark energy dynamics from supernovae, arXiv:1311.6678.

[87] David Benisty, Jurgen Mifsud, Jackson Levi Said, and Denitsa Staicova, On the robustness of the constancy of the Supernova absolute magnitude: Non-parametric reconstruction and Bayesian approaches, Phys. Dark Universe **39**, 101160 (2023).

[88] Rebecca Briffa, Salvatore Capozziello, Jackson Levi Said, Jurgen Mifsud, and Emmanuel N. Saridakis, Constraining teleparallel gravity through Gaussian processes, Classical Quantum Gravity **38**, 055007 (2020).

[89] Reginald Christian Bernardo, Daniela Grandón, Jackson Said Levi, and Víctor H. Cárdenas, Parametric and non-parametric methods hint dark energy evolution, Phys. Dark Universe **36**, 101017 (2022).

[90] Celia Escamilla-Rivera, Jackson Levi Said, and Jurgen Mifsud, Performance of non-parametric reconstruction techniques in the late-time universe, J. Cosmol. Astropart. Phys. 10 (2021) 016.

[91] Konstantinos Dialektopoulos, Jackson Levi Said, Jurgen Mifsud, Joseph Sultana, and Kristian Zarb Adami, Neural network reconstruction of late-time cosmology and null tests, J. Cosmol. Astropart. Phys. 02 (2022) 023.

[92] Daniel Foreman-Mackey, David W. Hogg, Dustin Lang, and Jonathan Goodman, emcee: The MCMC Hammer, Publ. Astron. Soc. Pac. **125**, 306 (2013).